Available online at www.sciencedirect.com

ScienceDirect

Earth and Planetary Science Letters 262 (2007) 563–580

EPSL

www.elsevier.com/locate/epsl

The lithium isotopic composition of orogenic eclogites and deep subducted slabs

Horst R. Marschall [a,*], Philip A.E. Pogge von Strandmann [a], Hans-Michael Seitz [b], Tim Elliott [a], Yaoling Niu [c]

[a] *Department of Earth Sciences, Wills Memorial Building, Queen's Road, University of Bristol, Bristol BS8 1RJ, UK*
[b] *J.W. Goethe Universität, Institut für Geowissenschaften, F.E. Mineralogie, Altenhöferallee 1, 60438 Frankfurt, Germany*
[c] *Department of Earth Sciences, Durham University, Science Labs, Durham DH1 3LE, UK*

Received 17 May 2007; received in revised form 7 August 2007; accepted 14 August 2007
Available online 21 August 2007
Editor: R.W. Carlson

Abstract

We have modelled the Li budget of subducting oceanic crust during dehydration, using recently established input parameters. The results show that the entire prograde metamorphic process, up to anhydrous eclogite, can account for a decrease in δ^7Li of only ≤3‰. Given that altered, oceanic crust entering the subduction zone should have Li isotopic compositions between −3 and +14‰, dehydration cannot account for markedly light Li isotopic compositions (δ7Li<0 to −10‰) previously measured in some high-pressure metamorphic (HPM) rocks. We have analysed another 41 orogenic HPM rocks from 11 different localities. These samples show a wide range in Li abundances from 1 to 77 μg/g. Li isotopic compositions of the rocks display both very heavy (δ^7Li>+6‰) and very light (δ^7Li<0‰) compositions, as low as −21.9‰. Notably some of the samples with highest Li concentrations are also isotopically light, which would not be predicted by isotopic fractionation as a consequence of Li loss during dehydration. Li abundances in excess of 30 μg/g in orogenic HPM rocks of basaltic composition (eclogites) are higher than any value of altered MORB and presumably result from addition of Li after the onset of subduction, most probably during eclogitisation or exhumation. Hence we propose that light-δ^7Li values are generated by kinetic fractionation of the Li isotopes during diffusive influx of Li from the country rocks into the exhuming eclogite bodies. Our conclusions are in stark contrast to the previously accepted model, as we predict the deeply subducted eclogites to have a Li isotopic signature heavier than the mantle.

Keywords: lithium isotopes; eclogite; high-pressure; modelling; subduction zone

1. Introduction

The light alkali metal lithium with its two stable isotopes, ^{6}Li and ^{7}Li, has gained significant attention among geochemists during the last decade. Moderate incompatibility during mantle melting, high mobility in hydrous fluids and a strong isotopic fractionation at low temperatures make this trace element a potentially powerful tracer for recycled material in the Earth's mantle (Zack et al., 2003; Tomascak, 2004; Elliott et al., 2004, 2006). Lithium is enriched in low-temperature oceanic crust with an increase of ^{7}Li/^{6}Li ratios (noted as δ^7Li, the deviation from the L-SVEC standard in permil) due to the interaction with the heavy-Li seawater (Donnelly et al., 1980; Ryan and Langmuir, 1987; Chan and Edmond,

---

[*] Corresponding author. Tel.: +44 117 3315006; fax: +44 117 9253385.
E-mail address: Horst.Marschall@bristol.ac.uk (H.R. Marschall).

doi:10.1016/j.epsl.2007.08.005

1988; Chan et al., 1992, 2002a; Moriguti and Nakamura, 1998; Tomascak et al., 2000). Rocks entering subduction zones, therefore, have heavy Li isotopic signatures relative to fresh MORB. Hence, fluids released from subducting slabs, infiltrating the overlying mantle, should also contain heavy Li. The relatively low temperatures at which subduction zone dehydration occurs, allow for stable isotope fractionation between metamorphosed rocks and released fluids. This process makes the slab-derived fluids yet heavier, as ^{7}Li is preferentially partitioned into the hydrous fluids. Tomascak et al. (2000) emphasised that the fractionation processes taking place in subducting slabs are important for understanding the Li isotopic compositions of island arc volcanic rocks, but the quantification of the element and isotope budgets of deeply subducted slabs are also essential for a prediction on the impact of subduction on the generation of mantle heterogeneities and global recycling.

Zack et al. (2003) presented a pioneering study on the alpine eclogites from Trescolmen (Switzerland) that provided the first Li isotope data on high-pressure metamorphic rocks. These authors reported extremely light δ^7Li-values in these rocks that were interpreted as the high-pressure equivalents of low-temperature altered basalts. Zack et al. argued that these low δ^7Li-values were the result of Li isotope fractionation during subduction dehydration. These findings have been a key in developing current models of geochemical cycling of Li in the mantle and the interpretation of δ^7Li signatures in mantle-derived magmatic rocks. However, no further investigation of Li isotopes in such rocks has so far been conducted.

Zack et al. (2003) presented their subducted light-Li hypothesis with clearly articulated caveats: (i) the Rayleigh dehydration modelling was completed on the basis of poorly-known parameters, i.e. Li partition coefficients and Li isotope fractionation between solids and fluids, and (ii) the samples came from a single locality and it is questioned how representative the Trescolmen eclogites are of subducting oceanic crust in general. Recently, Wunder et al. (2006, 2007) have completed a series of experimental studies on Li isotope fractionation between different silicates and hydrous fluids of variable composition at a wide range of temperatures. Marschall et al. (2007) have modelled the release of Li from dehydrating subducting crust based on mineral–mineral and mineral–fluid partition coefficients from earlier studies, in combination with petrologic modelling of the metamorphic phase transitions and the resulting fluid loss. With the parameters from these studies it is now possible to put the Li isotope fractionation model of dehydrating slabs on a sounder basis. Additionally, we analysed the Li isotope ratios of a large number of different high-pressure metamorphic rocks from a variety of localities and compared these results to the now larger set of data on altered oceanic crust, sediments and serpentinites. By including the new experimental data into modelling, we demonstrate that Li isotope ratios in subducting crust cannot be shifted significantly by dehydration. Hence, the extremely light Li observed in orogenic eclogites is not a result of prograde dehydration of altered oceanic crust. We argue that Li is mobilised and redistributed among different lithologies at depth and isotopically fractionated due to kinetic effects. Li isotope fractionation during diffusion has been shown to produce extremely light Li on various scales (Richter et al., 2003; Lundstrom et al., 2005; Teng et al., 2006; Jeffcoate et al., 2007; Parkinson et al., 2007) and may well have also operated in orogenic eclogite bodies.

2. Analytical methods

Li isotope analyses were made in both Bristol and Frankfurt and although similar approaches were used, details of the different procedures are given separately below.

2.1. Frankfurt

Samples were dissolved in several steps using HF-HNO_3 and HCl, and finally dissolved in 5N HNO_3-methanol mixture (1:4 by volume). For column separation we followed the procedure of Seitz et al. (2004). Samples were finally taken up in 2% HNO_3 (10 ng/g solution) for measurement by the ThermoElectron®-Neptune multi-collector (MC) ICP-MS at the Institut für Mineralogie, Universität Frankfurt. Analyses corrected for total analytical blanks agreed with the uncorrected analyses within ±0.6‰, 2σ. Analyses were carried out sequentially by "bracketing" the sample with the L-SVEC standard solution (10 ng/g), followed by a blank-measurement. The internal precision and long term external reproducibility is ~1.2‰. Repeat measurements of JB-2 yielded values of 5.2±1.2‰. Li isotopic compositions are given in delta values relative to the NIST L-SVEC standard (Flesch et al., 1973).

2.2. Bristol 1

Initially, samples at Bristol were analysed following the method of Jeffcoate et al. (2004), which is similar to the Frankfurt procedure. In brief, samples were dissolved using several steps of HF-HNO_3–$HClO_4$ and HCl. Li was separated from 10–25 mg aliquots of powder using a two step, dilute HNO_3-methanol/dilute

HCl-methanol chemistry and analysed by a sample-standard bracketing technique using a ThermoElectron®Neptune MC-ICP-MS. Samples were diluted to be within ±10% of the intensity of the NIST L-SVEC standard. The internal precision is <0.3‰. In the course of this study, inadvertent use of a 'dirty' batch of methanol containing some residual Ca induced poorer sample reproducibility than has been typical. For example, repeat analyses within the same analytical session varied by up to ±0.4‰, which compares unfavourably with our long term external reproducibility of ±0.3‰ (Jeffcoate et al., 2004). Such poorer reproducibility, however, is insignificant in the context of this study and notably full sample repeats using this method and a modified procedure (below) agree to within ±0.3‰ (Table 1). Concentrations were determined by intensity comparison with bracketing standard and have a precision of approximately ±10%.

2.3. Bristol 2

The problems outlined above lead us to try a chemical separation procedure that avoided methanol. We used a two-step high aspect-ratio cation exchange column method, with dilute HCl as an eluant based on the approach of James and Palmer (James and Palmer, 2000; Pogge von Strandmann et al., 2006). The very small sample sizes that can now be measured by MC-ICP-MS allow the dilute HCl procedure to be used effectively without risk of overloading the columns (c.f. Chan et al., 2002b). This technique provided a faster throughput of samples, that nevertheless yielded Li isotope ratios for standards consistent with our previous procedure. For the standards relevant to this study we obtained 5.0±0.3‰ (2 SD external error) for JB-2 (n=14, 11 dissolutions) and 4.8±0.2‰ for BHVO-2 (n=15, 11 dissolutions), using the same mass-spectrometric protocols as outlined in Jeffcoate et al. (2004).

3. Investigated samples

Eclogites and other high-pressure metamorphic (HPM) rocks form during metamorphism at high-P conditions at relatively low T. The low geothermal gradient required for the formation of blueschists and low-T eclogites is realised only in subduction zones, and eclogites are therefore thought to probe subducted crust. Classical localities in Europe and Asia display eclogites formed by subduction of mafic intrusives in continental crust, or by subduction of basaltic oceanic crust (C and O, respectively, in Table 1). In this study, we investigated 41 orogenic HPM rocks, including 29 eclogites, 5 meta-plagiogranites, 6 blueschists (including 3 clinopyroxene-bearing garnet+glaucophane-dominated metabasites), and one metarodingite. Samples were taken from Cima di Gagnone, Alpe Arami and Trescolmen in the Swiss Alps, from the Münchberg Complex (Variscan Fichtelgebirge, Bohemian Massif, Germany), from Aldalen in the Western Gneiss Region (=WGR, Norway), from the Greek island of Syros, from the North Qaidam and the East Qaidam (W China), from the Dabieshan and the Sulu complex (E China), and from the Tianshan (NW China). The meta-igneous HPM rocks from these localities are well characterised for their major, minor and trace elements and have been subject to many previous petrologic, geochronologic and geochemical studies. They are not only different in age and their spatial occurrence but also in their mineralogy and pressure-temperature history. A description of the samples and the geology of the localities are given in Appendix A.

4. Results

The investigated HPM rocks from all localities, together with the 9 eclogite samples investigated by Zack et al. (2003), show a wide range in Li abundances from ~1 to ~50 µg/g, with one sample exceeding 50 µg/g (Fig. 1; Table 1). Approximately 80% of all samples have Li concentrations between 5 and 25 µg/g (Fig. 1b), and the average eclogite Li concentration is 16.3±4.6 µg/g (2σ mean). Lithium isotopic composition of the rocks investigated in this study display an even larger range than the suite of Trescolmen eclogites from Zack et al. (2003). Both very heavy (δ^7Li>+6‰) and very light (δ^7Li<0‰) compositions were found. The lowest δ^7Li values were −21.9‰ for an eclogite sample from Daqaidam (Qaidam, China) and −18.2‰ for an eclogite sample from Cima di Gagnone (Swiss Alps). These extremely negative δ^7Li values are ~10‰ lower than the most negative values reported by Zack et al. (2003). However, the average eclogite δ^7Li value for all eclogite samples (including the nine eclogites from Zack et al., 2003) is −1.6±2.0‰ (2σ mean), and the δ^7Li histogram (Fig. 1a) shows a strong peak between 0 and +4‰. It is also important to note that no correlation was found between Li concentration and Li isotopic composition of the rocks, neither among rocks from a certain locality nor among the full population of all samples. Many of the negative-δ^7Li samples show Li abundances exceeding 30 µg/g (Fig. 1c). This observation is contrary to the positive correlation between Li concentrations and δ^7Li values predicted by a Rayleigh dehydration process.

Table 1
Lithium abundances and lithium isotopic compositions of investigated samples

Rock type	Orogen	Locality (continental/ oceanic origin)	*T* (°C)	*P* (GPa)	Age of HPM (Ma)	Sample	Latitude, longitude	Mineral assemblage	Analytical protocol	δ^7Li (‰)	±2σ	[Li] µg/g	±2σ	Reference to sample
Rocks characterised by the assemblage Na-rich Cpx + Grt ("eclogites")														
MPG	Hellenides	Syros, Greece (O)	480±30	1.5±0.3	54 (80?)	SY1	37° 29′48″ N, 024° 55′43″ E	Qtz, Cpx, Grt, Pg, Gln, Rt	[1]	−4.8	0.2	9.68*	0.97	[4]
						SY8	37° 29′25″ N, 024° 55′35″ E	Qtz, Cpx, Phe	[1]	+3.5	0.4	5.58*	0.56	[4]
						SY308	37° 29′34″ N, 024° 54′01″ E	Qtz, Pg, Cpx, Grt, Gln, Ep	[1]	+6.9	0.3	5.02*	0.50	[4,5]
						SY415	37° 29′29″ N, 024° 55′32″ E	Qtz, Cpx, Phe, Grt. Ep	[1]	+3.6	0.2	5.62*	0.56	[4]
						SY415	(replicate**)		[2]	+3.7	0.1			
						SY431	37° 30′06″ N, 024° 55′33″ E	Qtz, Cpx, Pg, Grt, Ep, Ttn	[1]	−4.3	0.3	22.7*	2.3	[4]
Eclogite	Hellenides	Syros, Greece (O)	480±30	1.5±0.3	54 (80?)	SY109	37° 29′ N, 024° 55′ E	Cpx, Grt, Gln, Qtz, Phe, Pg, Ep, Rt	[2]	+2.9	0.2	6.05*	0.37	[4,5,6]
						SY323	37° 29′ 31″ N, 024° 54′ 55″ E	Cpx, Grt, Ep, Ttu	[1]	+3.1	0.3	45.8*	0.9	[4,5,6]
	WGR	Aldalen, Norway (C)	725±25	2.7	430	AL1	62° 05′50″ N, 006° 22′00″ E	Grt, Cpx, Rt	[1]	+2.9	0.3	5.95*	0.37	
	Variscides	Münchberg, Germany (C)	650	2.6±0.2	380	FG97-1	50° 07′49″ N, 011° 41′25″ E	Cpx, Grt, Qtz, Phe	[3]	−6.8	1.5	10.2	0.8	[6]
						FG158	50° 07′04″ N, 011° 41′69″ E	Cpx, Grt, Qtz, Rt, Ky, Phe	[3]	−5.4	2.0	17.1	0.9	[6]
						FG85912	50° 07′04″ N, 011° 41′69″ E	Cpx, Grt, Qtz, Rt, Ky	[3]	+2.9	1.2	16.1	0.6	
						FG85916	50° 07′04″ N, 011° 41′69″ E	Cpx, Grt, Qtz, Rt, Ky, Am, Pl(s)	[3]	+0.6	2.2	7.56	1.02	[6]
						FG85930	50° 07′04″ N, 011° 41′69″ E	Cpx, Grt, Qtz, Rt, Ky, Phe	[3]	−7.5	0.2	76.9	3.1	[6]
	Qaidam	Daqaidam, W China (C)	700±50 (?)	3.1±0.2 (?)	430	DCD-99P1B3	38° 00′23″ N, 094° 53′01″ E	Grt, Cpx, Qtz, Rt	[2]	−21.9	0.4	18.4	1.1	
						DCD-99P1B8	38° 00′23″ N, 094° 53′01″ E	Grt, Cpx, Qtz, Am	[2]	−4.3	0.1	16.7	1.0	
						DCD-99P1B10	38° 00′23″ N, 094° 53′01″ E	Grt, Cpx, Qtz, Rt, Phe	[2]	−6.1	0.2	10.8	0.7	
						DCD-99P1B14	38° 00′23″ N, 094° 53′01″ E	Grt, Cpx, Qtz, Rt	[2]	−3.8	0.3	14.6	0.9	
		Dulan, W China (C)	700±50	3.1±0.2	430	EQD-QD04-2	36° 36′21″ N, 098° 26′19″ E	Grt, Cpx, Phe, Rt, Qtz	[2]	+2.5	0.3	32.2	1.9	
	Dabieshan	Bixiling, China (C)	1000	>4.0	220	DB-BXL-5	30° 34′23″ N, 116° 06′53″ E	Cpx[†], Grt, Ilm, Py, Ap	[2]	+5.4	0.4	4.86	0.29	
	Sulu	Yangkou, China (C)	850	>3.0	220	SL-JN29-2	36° 15′32″ N, 120° 40′21″ E	Cpx, Grt, Rt, Am, Qtz	[2]	+1.7	0.5	19.0	1.1	
						SL-S94-59	36° 15′32″ N, 120° 40′21″ E	Cpx, Grt, Rt, Qtz	[2]	+0.1	0.2	23.2	1.4	
						SL-S97020	36° 15′32″ N, 120° 40′21″ E	Cpx, Grt, Rt	[2]	+3.5	0.5	6.16	0.37	

						SL-S97077	36° 15′32″ N, 120° 40′21″ E	Grt, Cpx, Rt, Phe	[2]	+1.8	0.3	1.39	0.08	
	Tianshan	China (O)	550±50	>2.7	230	TS-B1	42° 33′32″ N, 081° 20′42″ E	Grt, Cpx, Gln, Ep, Qtz, Rt, Ttn(s)	[2]	+0.6	0.4	11.6	0.7	
						TS-B2	42° 33′32″ N, 081° 20′42″ E	Grt, Cpx, Ep, Gln, Rt, Ttn(s)	[2]	+0.3	0.2	15.9	1.0	
						TS-B4e	42° 33′32″ N, 081° 20′42″ E	Grt, Cpx, Ep, Gln, Rt, Ttn(s)	[2]	+0.5	0.3	14.9	0.9	
						TS-C1	42° 33′32″ N, 081° 20′42″ E	Grt, Cpx, Ep, Gln, Rt, Ttn(s)	[2]	+0.5	0.3	9.26	0.56	
						TS-C2e	42° 33′32″ N, 081° 20′42″ E	Grt, Cpx, Gln, Ep, Qtz, Rt, Ttn(s)	[2]	+0.5	0.3	13.0	0.8	
	Alps	Trescolmen, CH (C)	600	2.4	40	TC1	46° 23′48″ N, 009° 10′34″ E	Cpx, Grt, Qtz, Rt, Am(s)	[3]	+1.2	2.9	17.3	0.7	[6]
		Alpe Arami, CH (C)	875±25	3.8±0.4	40	AA1	46° 13′49″ N, 008° 58′30″ E	Cpx, Grt, Rt, Ky	[3]	−3.1	1.0	4.38	0.45	[6]
						AA28	46° 13′43″ N, 008° 58′23″ E	Cpx, Grt, Rt, Ky	[1]	−0.8	0.3	18.2*	0.7	
		Cima di Gagnone, CH (C)	725±25	3.2±0.2	40	III.121	46° 19′40″ N, 008° 51′15″ E	Grt, Cpx, Ky, Rt, Am, Ep	[3]	−18.2	0.2	30.7	1.4	
						III.122	46° 19′40″ N, 008° 51′15″ E	Grt, Cpx, Ky, Rt, Am, Ep	[3]	−9.7	0.4	1.81	0.04	
						163a.28	46° 19′40″ N, 008° 51′15″	Grt, Cpx, Ky, Rt, Am, Ep	[3]	−6.8	0.7	35.6	2.2	
MRod	Alps	Cima di Gagnone, CH (C)	725±25	3.2±0.2	40	CdG97IT	46° 19′40″ N, 008° 51′15″ E	Grt, Cpx (Di), Am, Ttn, Ep	[3]	+8.2	1.5	1.22	0.04	
Average “eclogite”										−1.6	2.0	16.3	4.6	
Concentration weighted average “eclogite”										−3.4				
Rocks dominated by the assemblage Gln + Grt (“blueschists”), some with prograde Cpx formation (“blueschist-eclogite”)														
BS-Ecl	Hellenides	Syros, Greece (O)	480±30	1.5±0.3	54 (80?)	SY344	37° 29′54″ N, 024° 55′28″ E	Cam, Gln, Cpx, Ep, Grt, Phe, Ttn	[1]	+0.7	0.2	18.8*	0.4	[4,5]
						SY425G	37° 29′32″ N, 024° 54′56″ E	Gln, Ep, Phe, Grt, Cpx, Qtz, Rt	[1]	−3.1	0.4	40.5*	0.3	[4]
						SY425G	(replicate**)		[2]	−2.5	0.4			
						SY342	37° 29′52″ N, 024° 55′22″ E	Gln, Grt, Ep, Cpx, Pg	[1]	+9.5	0.2	27.4*	0.6	[4]
Blueschist	Hellenides	Syros, Greece (O)	480±30	1.5±0.3	54 (80?)	SY3	37° 29′46″ N, 024° 55′40″ E	Gln, Grt, Qtz, Phe, Ep	[1]	+9.1	0.3	36.9*	0.2	[4]
						SY5	37° 29′25″ N, 024° 55′34″ E	Gln, Grt, Qtz, Ep, Rt, Ttn, Chl	[1]	+3.1	0.2	42.6*	1.4	[4]
						SY306	37° 29′34″ N, 024° 54′01″ E	Gln, Ep, Cld, Phe, Chl, Grt, Qtz	[1]	+8.7	0.4	7.14*	0.87	[4]
Average BS + BS-Ecl										+4.7	4.3	29.0	11.3	
Concentration weighted average BS + BS-Ecl										+3.9				

MPG = meta-plagiogranite (Cpx-Qtz-rich rocks of trondjemitic composition); MRod = metarodingite; BS-Ecl = rocks with modal composition transitional between blueschist and eclogite.

O and C refer to different settings for the protoliths of the HPM rocks: O = oceanic crust; C = mafic intrusions in or volcanic rocks erupted on continental crust. Mineral abbreviations after Kretz (1983). * Li concentrations measured by ICP-AES, all others by MC-ICP-MS. ** repeats of the entire chemical and MC-ICP-MS procedure, using a different protocol for column chemistry. † clinopyroxene grains show small symplectites at their rims. CH = Switzerland. Analytical protocols from: [1] = Jeffcoate et al. (2004); [2] = Pogge von Strandmann et al. (2006); [3] = Seitz et al. (2004). References are: [4] = Marschall (2005); [5] = Marschall et al. (2006a); [6] = Woodland et al. (2002).

5. Modelling of Li isotopes during fluid release

5.1. Metamorphic dehydration

The lithium isotopic composition of the subducting slab is modelled making three assumptions: (i) equilibrium between rock and fluid is achieved before the fluid is expelled; (ii) no external fluids are in contact with the rocks; (iii) no lithium is introduced into the rock during subduction. We later exmine these assumptions in the light of model results. In a first step, we modelled the loss of lithium from subducting rocks, employing a Rayleigh dehydration model similar to Zack et al. (2003), but using recently revised values for Li rock–fluid partitioning $D_{\mathrm{Li}}^{\mathrm{rock/fluid}}$ and Li isotope fractionation factors α (Fig. 2). Depending on the initial H_2O content, between 5 and 40% of the Li is lost from the rocks, while the δ^7Li-values are decreased by less than 5‰ (Fig. 3a). Notably, Li in the fully dehydrated eclogites is still heavier than Li in unaltered MORB.

On the basis of petrologic and thermobarometric studies, lithium loss has also been modeled by using a set of batch dehydration events leading from fully hydrated basalts (~5.5 wt.% H_2O) to phengite-bearing and dry eclogites by step-wise dehydration (Marschall et al., 2007). H_2O contents were calculated from the mineral parageneses that are stable along a P–T path derived from geophysical modelling. Values for $D_{\mathrm{Li}}^{\mathrm{rock/fluid}}$ are variable along the P–T path (Fig. 2a) and are calculated from mineral/fluid partition coefficients combined with the modal abundances of the minerals in the rocks, as derived from the petrologic calculations. By using this inclusive approach, a loss of 40 to 50% of the initial lithium was estimated (Marschall et al., 2007).

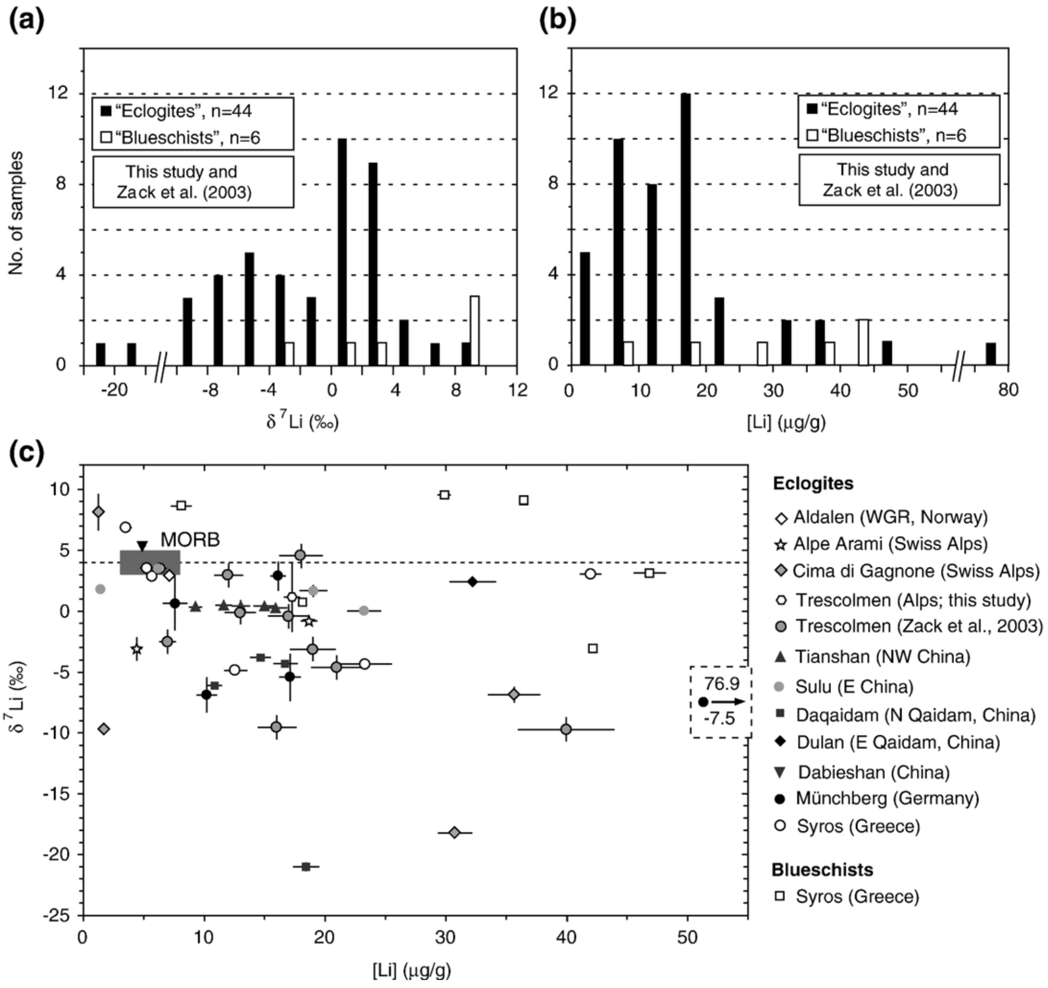

Fig. 1. Results of Li analyses of all high-pressure metamorphic rock samples (this study and Zack et al., 2003). (a) Histogram of δ^7 Li values of eclogites and blueschists. (b) Histogram of Li abundances of eclogites and blueschists. (c) Lithium concentration vs. lithium isotopic composition. Fresh MORB is represented by the grey box.

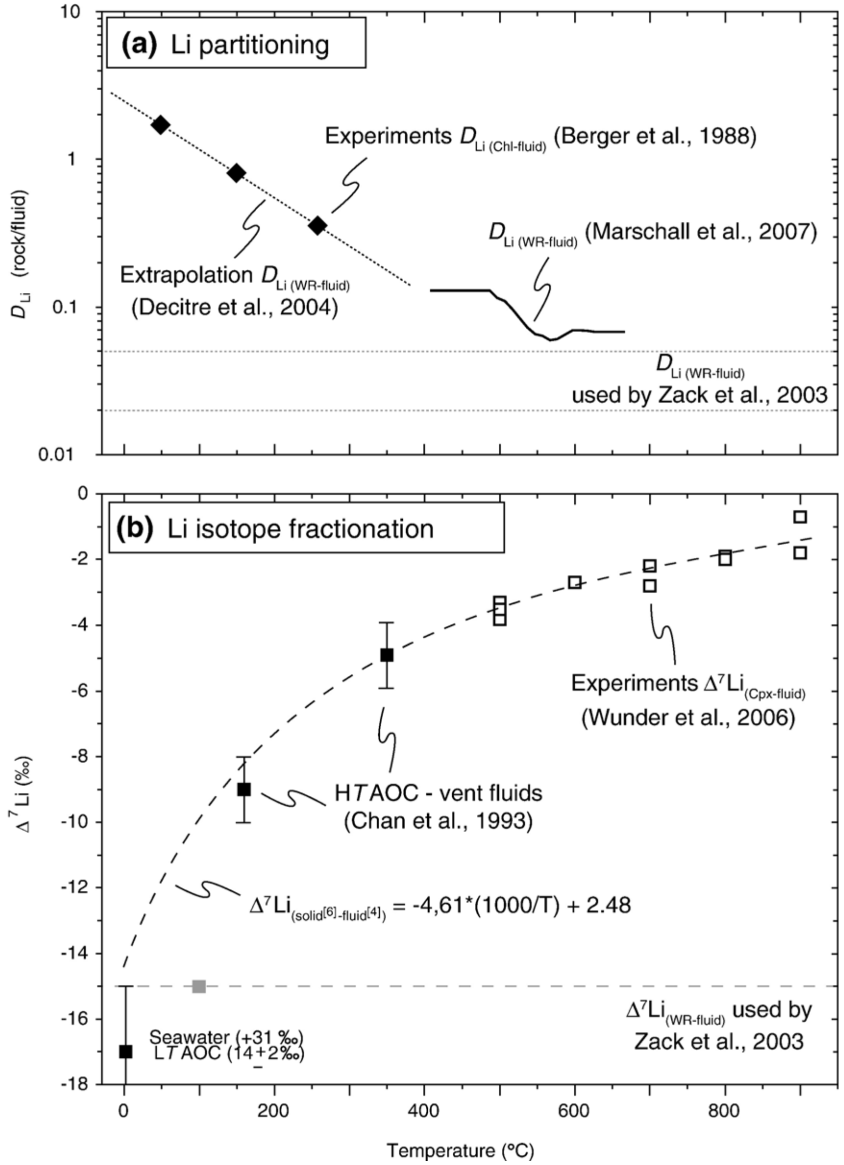

Fig. 2. (a) Li partitioning and (b) Li isotope fractionation between solids and fluid as a function of T, used for dehydration modelling. Data from different sources as given.

In addition, this model provides information on the T and P at which the consecutive portions of lithium and fluids are released. This enables us to include the temperature dependence of isotopic fractionation of stable isotopes, and to estimate the depths at which certain portions of fluids with their characteristic elemental and isotopic signatures are released (Table 2; Fig. 3b). The model was successfully applied for the evolution of boron isotopes before (Marschall et al., 2007) and is applied here for lithium isotopes.

Namely, Wunder et al. (2006, 2007) recently completed experimental studies on the lithium isotopic equilibrium fractionation between hydrous fluids (basic and acidic) and clinopyroxene ($\mathrm{Li^{VI}}$), mica ($\mathrm{Li^{VI}}$) and staurolite ($\mathrm{Li^{IV}}$). The experiments were conducted at various temperatures between 300 and 900 °C. As predicted by theory, the results show a negative correlation between Li isotope fractionation and temperature (Fig. 2b). For clinopyroxene the fractionation $\Delta^7\mathrm{Li}_{\mathrm{Cpx-fluid}} = \delta^7\mathrm{Li}_{\mathrm{Cpx}} - \delta^7\mathrm{Li}_{\mathrm{fluid}}$ is given as

$$\Delta^7\mathrm{Li}_{\mathrm{Cpx-fluid}} = -4.61(1000/T(K)) + 2.48. \qquad (1)$$

The extrapolation of the results to lower temperatures is in good agreement with estimates from studies on

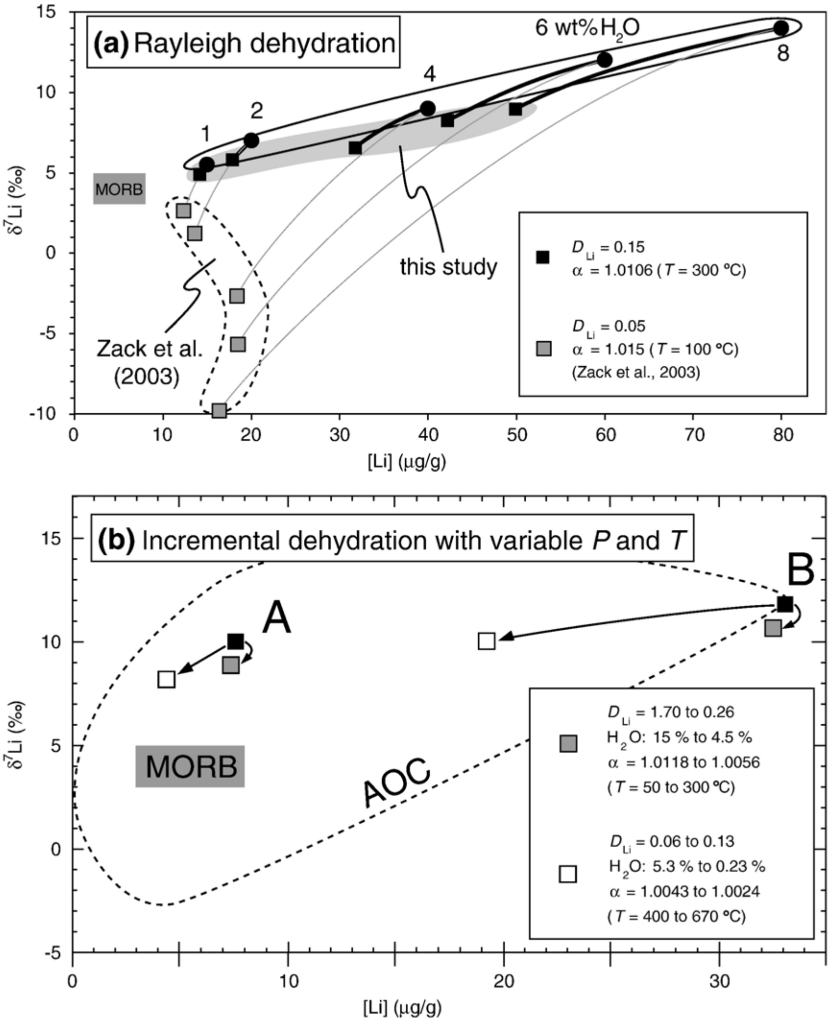

Fig. 3. Modelled Li evolution of dehydrating oceanic crust. (a) Rayleigh dehydration model with two different sets of input parameters. Black lines and squares: this study as discussed in text (the grey field represents the dehydrated eclogite compositions); grey lines and squares: Zack et al. (2003) with the dashed line enclosing their eclogite field. (b) Incremental dehydration model with D and α values changing as a function of T Marschall et al. (2007). A: average altered oceanic crust; B: highly altered oceanic crust. Black squares represent the initial compositions. White squares represent the modelled eclogite compositions after metamorphic dehydration. Grey squares represent the modelled composition of AOC after low-T dehydration and diagenesis. The dashed loop encloses the vast majority of published compositions of AOC samples. Note the different scales of (a) and (b).

natural fluid–rock sample pairs (Chan et al., 1992, 1993, Fig. 2). The determined Li isotope fractionation between minerals and fluids is much smaller than the fractionation of B isotopes, and results in values for $\Delta^7\mathrm{Li}_{\mathrm{Cpx-fluid}}$ of −5.6‰ at 300 °C and −2.3‰ at 700 °C. Fractionation between mica and fluid as well as staurolite and fluid is yet smaller (Wunder et al., 2007). Hence, the Li isotopic fractionation at temperatures typical for metamorphic reactions in subducting slabs is less than previously thought. However, the well-determined temperature-dependent isotope fractionation can be used in combination with the recently modelled Li loss during dehydration to estimate more rigorously the Li isotopic composition of subducting oceanic crust.

Published Li abundances and isotopic ratios of natural AOC samples are taken as initial values in the model. They range from <1 µg/g Li and $\delta^7\mathrm{Li} \approx 0$‰ for high-$T$ altered basalts to 33 µg/g Li and $\delta^7\mathrm{Li} = +14$‰ for low-$T$ altered portions of oceanic crust, with most samples containing <20 µg/g Li (Fig. 4b). Higher Li abundances in strongly altered basaltic breccias and hyaloclastites (6–56 µg/g Li; 1 sample 79 µg/g) are reported (with no Li isotope values given) in one early study on AOC from DSDP Leg 51, site 417 (Donnelly et al., 1980). Chan et al. (2002a) calculated a weighted

Table 2
Input parameters and results of modelling of Li concentrations and Li isotopic compositions of solids and fluids during low-*T* fluid loss and metamorphic dehydration of AOC

					Average AOC (A)				Highly altered AOC (B)			
T (°C)	P (GPa)	H_2O (wt %)	D_{Li} solid-fluid	Δ^7 Li (%)	[Li] solid (μg/g)	[Li] fluid (μg/g)	δ^7 Li solid (%)	δ^7 Li fluid (%)	[Li] solid (μg/g)	[Li] fluid (μg/g)	δ^7 Li solid (%)	δ^7 Li fluid (%)
Low-temperature fluid loss												
50	0.04	15.00	1.699	−11.79	7.60		+10.00		33.1		+11.80	
55	0.05	14.60	1.637	−11.57	7.61	4.65	+9.97	+21.54	33.2	20.3	+11.77	+23.34
60	0.06	14.20	1.576	−11.36	7.63	4.84	+9.93	+21.29	33.2	21.1	+11.73	+23.09
65	0.07	13.80	1.518	−11.15	7.64	5.03	+9.90	+21.05	33.3	21.9	+11.70	+22.85
70	0.08	13.40	1.463	−10.95	7.65	5.23	+9.87	+20.82	33.3	22.8	+11.67	+22.62
75	0.09	13.00	1.409	−10.76	7.66	5.44	+9.83	+20.59	33.4	23.7	+11.63	+22.39
80	0.10	12.60	1.357	−10.57	7.67	5.65	+9.80	+20.37	33.4	24.6	+11.60	+22.17
85	0.11	12.20	1.307	−10.39	7.68	5.87	+9.76	+20.15	33.4	25.6	+11.56	+21.95
90	0.13	11.80	1.259	−10.21	7.68	6.10	+9.72	+19.94	33.5	26.6	+11.52	+21.74
95	0.14	11.40	1.213	−10.04	7.69	6.34	+9.69	+19.73	33.5	27.6	+11.49	+21.53
100	0.15	11.00	1.168	−9.87	7.70	6.59	+9.65	+19.52	33.5	28.7	+11.45	+21.32
105	0.16	10.49	1.125	−9.71	7.70	6.85	+9.60	+19.31	33.5	29.8	+11.40	+21.11
110	0.17	9.98	1.083	−9.55	7.70	7.11	+9.55	+19.10	33.6	31.0	+11.35	+20.90
120	0.18	8.96	1.005	−9.25	7.70	7.66	+9.45	+18.69	33.6	33.4	+11.25	+20.49
130	0.20	7.94	0.933	−8.95	7.70	8.26	+9.34	+18.30	33.5	36.0	+11.14	+20.10
140	0.25	6.92	0.865	−8.68	7.69	8.88	+9.23	+17.91	33.5	38.7	+11.03	+19.71
150	0.33	6.41	0.803	−8.41	7.68	9.56	+9.18	+17.59	33.4	41.6	+10.98	+19.39
175	0.50	5.90	0.665	−7.81	7.65	11.5	+9.11	+16.92	33.3	50.1	+10.91	+18.72
200	0.66	5.76	0.552	−7.26	7.65	13.9	+9.09	+16.36	33.3	60.4	+10.89	+18.16
220	0.79	5.62	0.475	−6.87	7.63	16.1	+9.07	+15.94	33.2	70.0	+10.87	+17.74
240	0.92	5.48	0.409	−6.50	7.62	18.6	+9.05	+15.55	33.2	81.2	+10.85	+17.35
260	1.06	5.20	0.352	−6.17	7.57	21.5	+9.00	+15.17	33.0	93.8	+10.80	+16.97
280	1.19	4.78	0.303	−5.85	7.50	24.8	+8.91	+14.77	32.7	108	+10.71	+16.57
300	1.32	4.50	0.261	−5.56	7.44	28.5	+8.85	+14.42	32.4	124	+10.65	+16.22
Metamorphic dehydration												
407	1.62	5.27	0.129	−4.30	7.60		+10.00		33.1		+11.80	
417	1.64	5.26	0.129	−4.20	7.60	59.0	+10.00	+14.20	33.1	257	+11.80	+16.00
427	1.65	5.26	0.129	−4.11	7.59	59.0	+9.99	+14.10	33.1	257	+11.79	+15.90
437	1.67	5.25	0.129	−4.01	7.59	58.9	+9.99	+14.01	33.0	257	+11.79	+15.81
447	1.69	5.23	0.129	−3.92	7.58	58.8	+9.99	+13.91	33.0	256	+11.79	+15.71
457	1.71	5.23	0.129	−3.84	7.58	58.7	+9.99	+13.82	33.0	256	+11.79	+15.62
467	1.73	5.22	0.129	−3.75	7.57	58.6	+9.98	+13.73	33.0	255	+11.78	+15.53
477	1.75	5.21	0.129	−3.67	7.57	58.6	+9.98	+13.65	33.0	255	+11.78	+15.45
487	1.77	5.20	0.129	−3.59	7.56	58.5	+9.98	+13.56	32.9	255	+11.78	+15.36
497	1.79	4.09	0.115	−3.51	6.94	60.5	+9.65	+13.16	30.2	263	+11.45	+14.96
507	1.82	3.63	0.109	−3.43	6.68	61.1	+9.51	+12.94	29.1	266	+11.31	+14.74
517	1.85	2.61	0.096	−3.36	6.08	63.3	+9.18	+12.53	26.5	276	+10.98	+14.33
527	1.88	2.23	0.084	−3.28	5.84	69.5	+9.03	+12.32	25.4	303	+10.83	+14.12
537	1.91	1.99	0.072	−3.21	5.66	78.4	+8.93	+12.14	24.6	341	+10.73	+13.94
547	1.94	1.80	0.065	−3.14	5.50	84.3	+8.84	+11.98	24.0	367	+10.64	+13.78
557	1.98	1.65	0.064	−3.07	5.38	84.7	+8.76	+11.84	23.4	369	+10.56	+13.64
567	2.02	1.39	0.059	−3.01	5.17	87.0	+8.64	+11.64	22.5	379	+10.44	+13.44
577	2.07	1.23	0.061	−2.94	5.04	83.2	+8.56	+11.50	22.0	363	+10.36	+13.30
587	2.12	1.00	0.065	−2.88	4.88	75.2	+8.46	+11.34	21.2	327	+10.26	+13.14
597	2.17	0.77	0.069	−2.82	4.73	68.2	+8.37	+11.19	20.6	297	+10.17	+12.99
607	2.22	0.45	0.070	−2.76	4.53	65.2	+8.25	+11.00	19.7	284	+10.05	+12.80
617	2.28	0.31	0.069	−2.70	4.45	64.9	+8.19	+10.89	19.4	283	+9.99	+12.69
627	2.34	0.23	0.068	−2.64	4.40	65.0	+8.16	+10.81	19.2	283	+9.96	+12.61
667	2.64	0.23	0.068	−2.42	4.40	65.0	+8.16	+10.59	19.2	283	+9.96	+12.39

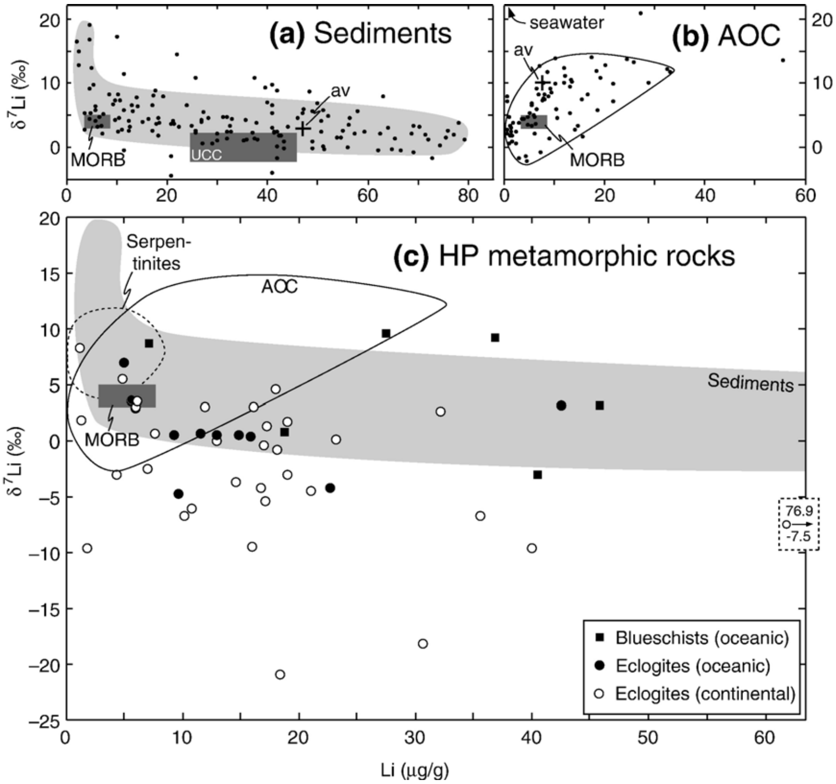

Fig. 4. Lithium concentration vs. Li isotopic composition of natural samples. (a) Published analyses of world wide seafloor sediments (Chan et al., 1992, 1994; Bouman et al., 2004; Chan et al., 2006; James et al., 1999). Grey boxes represent compositions of MORB and upper continental crust (UCC, Teng et al. (2004)). The cross locates the weighted average of global seafloor sediments at subduction zones Chan et al. (2006). (b) Altered magmatic rocks of the oceanic crust (AOC) (Chan et al., 1992, 2002a; Bouman et al., 2004; Chan et al., 2006; Clift et al., 2005), with weighted average (Chan et al., 2002a) marked by the cross. (c) high-pressure metamorphic rocks (Zack et al., 2003, and this study). Grey box represents fresh MORB; grey field represents the majority of sediments (from panel a); solid loop represents the majority of AOC samples (from panel b); dashed loop encloses serpentinised abyssal peridotites (Decitre et al., 2002).

average of the upper volcanic layer of the oceanic crust (Layer 2A) by integrating ODP core samples to be 7.6 μg/g Li with an isotopic composition of δ^7Li= +10.0‰.

Two different initial AOC compositions were chosen in the models to span the range of possible inputs: (A) average AOC with [Li]=7.6 μg/g and δ^7Li=+10.0‰, and (B) highly altered AOC with [Li]=33.1 μg/g and δ^7Li=+11.8‰ (Table 2; Fig. 3b). Calculations were performed using the hydrated MORB composition and dehydration reactions given in Marschall et al. (2007), resulting in 42% of the initial Li lost during eclogite formation. Note, that this value is constrained by the sequence of metamorphic reactions and the value of $D_{\mathrm{Li}}^{\mathrm{rock/fluid}}$ as a function of P and T (Table 2; Fig. 2a), as determined by a combination of experimental results and analyses of natural samples (Brenan et al., 1998; Marschall et al., 2006a, 2007).

Modelled concentrations of lithium for the fully dehydrated eclogites are 4.4 μg/g in case A (average AOC) and 19.2 μg/g in case B (Table 2; Fig. 3b). The fractionation of ^{7}Li into the fluid leads to decreasing δ^7Li values of the HPM rocks and of the released fluids with increasing depth. However, the relatively small fractionation factor at metamorphic temperatures restricts this effect to only ~2‰ for the entire dehydration process. The eclogite of case A has a δ^7Li value of +8.2‰. The eclogite of case B has a δ^7Li value of +10.0‰ (Fig. 3b). Fluids released during dehydration of average AOC (case A) contain between 59 and 87 μg/g Li with δ^7Li values decreasing from +14.2 to +10.6‰ (Table 2).

The model used is based on a relatively hot P–T path (Marschall et al., 2007), leading to dehydration at relatively shallow depths. During cold subduction, hydrous minerals remain stable to greater depth, due to a positive Clapeyron slope of most dehydration reaction curves. This leads to the remarkable fact that dehydration takes place at higher temperature during colder subduction. Equilibrium stable isotope fractionation during dehydration is, therefore, less pronounced in slabs following colder *P*–*T* paths. It is also less pronounced in deeper layers of the slab than at its surface, because most dehydration reactions occur at higher *P* and *T* in the deeper layers.

As demonstrated above, metamorphic dehydration in the temperature range between 400 and 670 °C during the transformation from greenschist to blueschist to eclogite leads to a decrease of the Li isotopic composition of less than 3‰ (Fig. 3b). The process is, therefore, not sufficient to explain negative δ^7Li values of eclogites or even compositions as light as MORB (~+4‰) starting from average or highly altered oceanic crust (Fig. 3b).

5.2. Low-temperature fluid loss during diagenesis and early metamorphism

Isotopic fractionation at low temperatures typical for diagenetic and very low-grade metamorphic processes is much more pronounced than at temperatures typical for blueschist-to-eclogite transition. Therefore, it has been argued that de-watering and fluid loss at the onset of subduction at low temperatures could strongly fractionate the Li isotopes and be responsible for a significant decrease of δ^7Li values in the subducting slab (Zack et al., 2003). Highly altered basalts rich in clay minerals (smectite), chlorite and zeolites may also show high H_2O contents of >15 wt.%. Such a strong alteration not only increases the amount of H_2O and Li in the rocks, but it has also an impact on other elements, producing for example an increase in K, Na, Fe and Mn contents, an increase of the Fe^{3+}/Fe ratio, a shift in SiO_2 contents, and the formation of a Ce anomaly. The HPM equivalents of such highly altered basalts would mirror those deviations from basaltic compositions. High modal abundances in white mica, Fe-oxides and apatite along with the chemical changes make those HPM rocks readily identifiable and distinguishable from "normal" eclogites, which evolved from protoliths that were only moderately altered on the seafloor. In any case, clay minerals and zeolites become unstable at the onset of metamorphism, and large amounts of fluid are released at low temperatures. It is probably not possible to present a fully quantitative model of the effects of diagenesis and early metamorphism, due to non-equilibrium reactions, mineral surface effects and the general lack of experimental equilibrium data for those conditions. However, the impact of low-temperature processes on the Li isotopes can be approximated, as demonstrated below.

The extrapolation of Eq. (1) to lower temperatures reveals $\Delta^7\text{Li}_{\text{solid-fluid}}$ values of −7.3‰ for 200 °C and −14.3‰ for 2 °C (Fig. 2b). The upper limit of the δ^7Li value of +14‰ for AOC in contact with seawater ($\delta^7\text{Li} \approx +31$‰) suggests a $\Delta^7\text{Li}_{\text{solid-fluid}}$ value of −17‰ for conditions at the ocean floor (~2 °C) (Chan et al., 1992, Fig. 2b). Experiments on the Li isotopic fractionation between smectite–illite and hydrothermal fluids at 300 °C revealed $\Delta^7\text{Li}_{\text{solid-fluid}}$ values between −0.2 and −11.6‰, depending on the grain size of the clay minerals (Williams and Hervig, 2005). The ratio of Li incorporated into octahedral sites of the crystal lattice to Li on interlayer sites probably causes the grain-size effect (Williams and Hervig, 2005).

The elemental partitioning of Li between minerals (chlorite, smectite and zeolite) and hydrothermal solutions has been investigated experimentally at temperatures between 50 and 300 °C (Berger et al., 1988). Li partitions into the solids at low temperatures with smectite and zeolite showing $D_{\text{Li}}^{\text{solid/fluid}}$ values between 1.9 and 33, i.e. above unity over the entire temperature range. The $D_{\text{Li}}^{\text{chlorite/fluid}}$ value for chlorite is also above 1 at low temperatures and drops below 1 at $T \approx 120$ °C (Fig. 2b). The experimental data from Berger et al. (1988) was used and extrapolated by Decitre et al. (2004) (Fig. 2b) to model the Li exchange during low-*T* hydrothermal alteration of seafloor sediments.

Another experimental study (Chan et al., 1994), investigating the Li mobilisation in natural sediments revealed strong retention of Li in the solids during progressive heating. In this study, the Li concentrations in the fluids increased steadily from 0.05 to 16 µg/g in contact with sediment containing ~70 µg/g Li, as the temperature was increased from 25 to ~350 °C (Chan et al., 1994). Upon cooling from ~350 to 25 °C, the Li concentration remained more or less constant between 20 and ~30 µg/g in contact to sediment that contained 20.3 µg/g Li at the end of the experiment (Chan et al., 1994). Note, that the observed mobilisation of 73% of the Li from the rocks (Chan et al., 1994) is only obtained by a high fluid/rock ratio of 3. During dehydration without an external flux of fluid, however, the fluid/rock ratio is significantly lower (~0.01 to 0.2).

All the experiments demonstrate that Li mobilisation from sediments and clay-rich altered basalts is ineffective at temperatures below 250 °C (Berger et al., 1988; Chan et al., 1994, 1999). The partitioning of Li into the solid phases at these temperatures is consistent with its strong enrichment in low-*T* AOC (7.6 µg/g) during interaction with seawater (0.18 µg/g). The high $D_{\text{Li}}^{\text{rock/fluid}}$ during low-temperature dehydration thus greatly limits the impact this process can have on the Li isotope composition of dehydrating rocks.

We modelled diagenetic (very low temperature) dehydration by using $\Delta^7\text{Li}_{\text{solid-fluid}}$ values derived from

Eq. (1) and the temperature-dependent $D_{\mathrm{Li}}^{\mathrm{rock/fluid}}$ value (Berger et al., 1988). H_2O contents decrease from 15 wt.% (50 °C, smectite dominated) to 7 wt.% (120 °C, illite–chlorite dominated) to 4.5 wt.% (300 °C, phengite–chlorite dominated). In natural samples, the H_2O contents may vary with the chemical and mineralogical composition of the rocks. However, this does not have a significant impact on the Li budget, due to the high partition coefficient of Li at low T. Accordingly, the model predicts a decrease of δ^7Li values in the rocks of only 1.1‰ with Li concentrations remaining at 98% of the initial levels. Composition A (average AOC) decreases to values of $\delta^7\mathrm{Li}=+8.9$‰ and [Li] = 7.4 μg/g, while composition B (highly altered AOC) reaches values of $\delta^7\mathrm{Li}=+10.7$‰ and [Li] = 32.4 μg/g at 300 °C (Table 2; Fig. 3b). Hence, fluid loss at very low temperatures may decrease the δ^7Li value of the rocks by only ~1‰, and can, therefore, not be responsible for light Li compositions in the subducting slab.

The fluids released in all modelled cases are Li-rich (Table 2). During the low-T dehydration of composition A (average AOC) concentrations increase with T from 4.7 μg/g (= 26 × seawater) at 50 °C to 28.5 μg/g (~160 × seawater) at 300 °C. Li in the fluids is heavy, decreasing from $\delta^7\mathrm{Li}=+21.5$‰ to +14.4‰ over the same temperature range (Table 2).

6. Discussion

6.1. Discrepancy between our model and the model of Zack et al. (2003)

Due to the lack of experimental data on Li isotope fractionation at metamorphic temperatures and poor data on Li partitioning, Zack et al. (2003) were forced to model Li loss and δ^7Li evolution during dehydration based on input parameters that were assumed to be reasonable. They chose a fixed value $D_{\mathrm{Li}}^{\mathrm{rock/fluid}}$ of 0.05 together with a fractionation factor α of 1.015, corresponding to ~15‰ fractionation between solids and fluids (Fig. 2). These input parameters result in a dramatic decrease of δ^7Li values during dehydration (Fig. 3). Furthermore, they argued that an even larger reduction in δ^7Li may be achieved during the breakdown of chlorite, assuming that values of $D_{\mathrm{Li}}^{\mathrm{rock/fluid}}$ may drop to 0.02 (Fig. 2a). However, as demonstrated above, dehydration at low temperatures (<300 °C) has a restricted impact on the Li budget of rocks, caused by the high Li partition coefficient $D_{\mathrm{Li}}^{\mathrm{solid/fluid}}$ of low-T minerals, such as smectite, illite, chlorite and zeolite. This leads to a strong retention of Li in the rocks and restricts the shift of δ^7Li values to ~1‰, only. At higher temperatures, the $D_{\mathrm{Li}}^{\mathrm{solid/fluid}}$ values decrease to ~0.1 in metabasic composition (Fig. 2a; Marschall et al., 2007), leading to a loss of approximately half of the initial Li from the rocks (Marschall et al., 2007). The very low $D_{\mathrm{Li}}^{\mathrm{rock/fluid}}$ value of 0.02 for chlorite breakdown proposed by Zack et al. (2003), however, is not achieved, because the product assemblages of the chlorite-breakdown reactions still include minerals that have high $D_{\mathrm{Li}}^{\mathrm{solid/fluid}}$ values, such as amphibole, clinopyroxene and white mica. Note, that chlorite breakdown is indeed included in the modelled reaction sequence (Marschall et al., 2007). The effect of Li loss on the Li isotopic composition of the rocks at temperatures >300 °C is restricted by the limited isotopic fractionation at these conditions (Fig. 2b). The experimentally determined $\Delta^7\mathrm{Li}_{\mathrm{solid-fluid}}$ values now available (Wunder et al., 2006, 2007) are smaller than previously thought, and limit the decrease of δ^7Li values during the greenschist to blueschist to eclogite transition to approximately 2‰ (Fig. 3b). A recent study by Teng et al. (2007) on a well-defined natural setting may be taken as evidence for the validity of our modelling results. These authors investigated a contact aureole of a granodiorite intrusion, and found a limited decrease of δ^7Li values (≤1.5‰ only) along with a loss of ~50% of the Li in the contact metamorphic rocks at $T \geq 500$ °C.

6.2. Discrepancy between modelled compositions and natural samples

Our model demonstrates that equilibrium dehydration is not a viable mechanism to explain the highly negative δ^7Li values observed in some eclogites. Even the more common MORB-like values (~4‰) cannot be obtained by dehydration of average AOC. It is, therefore, necessary to step back and question the modelling assumptions:

(i) It was assumed that Li isotopic equilibrium between rocks and fluid is obtained during dehydration. This is supported by the fact that Li diffuses very rapidly (Li and Gregory, 1974; Coogan et al., 2005) and by restricted variations in Li inter-mineral partition coefficients in dehydrated HPM rocks (Marschall et al., 2006a). However, it is possible that fluids are expelled without fully equilibrating with the restitic mineral assemblage. This would produce Li zonation in minerals with concentrations decreasing from core to rim, resulting from diffusive loss of Li from the rims of grains into the released fluid. The faster diffusion of 6 Li in comparison to ^{7}Li (Richter et al., 2003, 2006) would in that case deplete the minerals in ^{6}Li with respect to ^{7}Li. As a result, the dehydrated rocks would retain heavier Li than in the case of equilibrium dehydration, which translates to higher δ^7Li values.

(ii) Our second model assumption is that all fluid interacting with the rocks during progressive dehydration is derived internally from the breakdown of hydrous minerals, i.e. no external fluids are involved. This assumption restricts the fluid/rock ratio to ~0.01 to ~0.06 (by mass) for the metamorphic dehydration reactions and ~0.2 for low-temperature (diagenetic) de-watering. These numbers significantly increase when the rocks are fluxed by fluids from external sources. The transport of hydrous fluids through subducting oceanic crust at high pressures was recently demonstrated to be not dispersive, but rather focussed and channelised (John and Schenk, 2003; Ague, 2003, 2007; Zack and John, 2007). This leads to highly variable fluid/rock ratios within the subducting crust. Fluid channel zones may suffer strong interaction with external fluids (fluid flux $>10^4$ cm^3/cm^2; Ague, 2003; John et al., 2004; Zack and John, 2007), while the major part of the rock pile is not affected by strong fluid flux, but governed by dehydration. Rocks within the fluid channel zones are not only influenced in their trace element and isotopic composition, but also in their mineralogy and major element composition (Becker et al., 1999; Widmer and Thompson, 2001; Spandler and Hermann, 2006), and can thus be recognised in the field. Hence, the majority of high-pressure rocks with major-element compositions similar to their igneous protoliths are influenced by simple dehydration. Rocks that suffered flux from Li-poor external fluids would be leached and would display Li concentrations lower than those produced by dehydration alone. However, it still holds that only modest equilibrium isotopic fractionation occurs at such temperatures, limiting any decrease in δ^7Li. This scenario would result in rocks with very low Li abundances and moderately high δ^7Li values.

(iii) Our third assumption was that the Li found in the exhumed HPM rocks on the Earth's surface today represents the initial Li contained in the rocks before subduction, less the amount of Li released during dehydration. No Li is allowed to enter the rocks during subduction, high-pressure metamorphism or exhumation. However, Li abundances in AOC, the most likely protoliths of high-Li eclogites, range from <1 to ~20 μg/g (30 μg/g in a few cases; Fig. 4b) with a weighted mean of 7.6 μg/g (Chan et al., 2002a). These values are too low to account for many of the high Li concentrations found in exhumed orogenic eclogites. Most eclogite samples have Li contents significantly above the average AOC and more than 20% exceed 30 μg/g (Fig. 1b). Hence, arguing from the Li abundances alone, it is clear that the Li found in the eclogites cannot be solely attributed to Li remaining in the rocks from their pre-subduction stage. Orogenic eclogites must have gained Li during the subduction or exhumation process.

6.3. Lithium re-distribution at depth

Re-distribution of Li within the subducting slab is of lesser importance for models of global recycling and formation of mantle inhomogeneities, as the subducting slab as a whole remains unchanged by this process. However, a closer investigation of the Li source(s) and relative timing of re-distribution may contribute further insights into the mechanisms of slab-to-mantle Li transfer. Sources of trace elements in subducting slabs are generally assigned to the three major lithologies, igneous oceanic crust, serpentinites and sediments. As demonstrated above, fluids released from AOC at any depth or any metamorphic transition (equilibrium or disequilibrium) will always generate high-δ^7Li fluids with intermediate to high Li concentrations.

Serpentinites and serpentinised peridotites dredged or drilled from the ocean floor show relatively low Li whole-rock concentrations of 0.1 to <15 μg/g (Decitre et al., 2002; Niu, 2004; Scambelluri et al., 2004; Vils et al., 2007). Many peridotites indeed show a depletion of Li during serpentinisation (Vils et al., 2007). Lithium in abyssal serpentinite is heavy with whole-rock δ^7Li values of approximately +3 to +14‰ (Decitre et al., 2002). The breakdown of serpentinite during deep subduction would release hydrous fluids that are likely to interact with the overlying meta-igneous portion of the subducting slab and alter its trace-element budget (John et al., 2004; Schmidt et al., 2004; Zack and John, 2007) at least along the above-mentioned fluid transport veins (John and Schenk, 2003). However, the low Li concentrations in serpentinites together with a relatively high $D_{\mathrm{Li}}^{\mathrm{rock/fluid}}$ partition coefficient of ≥0.3 (Scambelluri et al., 2004) leads to a relatively low Li content in fluids released during serpentinite dehydration. Therefore, fluids released from serpentinite are most probably Li-poor with high δ^7Li values.

The most Li-rich rocks in the subducting slab at the onset of subduction are clay-rich sediments. Global seafloor sediments show a wide range of Li concentrations from ~1 to 80 μg/g and δ^7Li values ranging from 0 to +7‰ in most samples (Fig. 4a; Chan et al., 1994, 2006; James et al., 1999; Bouman et al., 2004). The global mass-weighted mean for sediments at the onset of subduction was estimated to be 43.3 μg/g Li with a δ^7Li value of +3.01‰ (Chan et al., 2006). Therefore, sediments are the most Li-rich reservoir in the oceanic lithosphere with the lightest δ^7Li value. The Li isotopic composition of continental sediments and sedimentary rocks may be best estimated from the value of the Upper Continental Crust (UCC) of $\delta^7\text{Li}=0\pm2$‰ with $[\text{Li}]=35\pm11$ μg/g (Teng et al., 2004). A comparison of Li abundances and isotopic compositions of HPM rocks ("eclogites") and seafloor sediments shows that a large number of HPM rocks have Li concentrations and δ^7Li values comparable to sediments and UCC (Fig. 4c), i.e. the majority of points lies outside the fields of AOC (and serpentinites). This encourages the idea that high Li abundances in eclogites are generated by Li transfer from sediments into meta-igneous rocks at depth. This hypothesis is supported by field observations. As described in Appendix A, many orogenic eclogites are found as lenses or layers within metasedimentary schists and gneisses that share at least part of the metamorphic history with the mafic lithologies. Hydrous mineral assemblages at the contact zones of eclogite lenses and host rocks, in addition to trace element and stable isotope studies have proven fluid exchange between the contrasting rock types for several localities (Bröcker and Enders, 2001; Wiesli et al., 2001; Zack et al., 2001, 2002; Marschall et al., 2006b; Zack and John, 2007).

In a classical oceanic crust pile, the sediments will be located on top of the subducting slab, and will thus be heated up faster and dehydrate earlier than the magmatic and ultramafic rocks in deeper levels. The released fluids will generally migrate upwards into the fore-arc or sub-arc mantle and will not in-filtrate the underlying meta-igneous rocks. Thus, it seems unlikely that Li is transferred from sediments into the meta-igneous layers within subducting oceanic crust, unless the former surface of the ocean floor is regarded, where pillow basalts are indeed interlayered with sediments. The exhumation of orogenic eclogites, however, requires them to travel tens of kilometres from depth back to the surface. Field relations in some orogenic terrains (e.g. Syros) show meta-igneous blocks enclosed in mafic–ultramafic schists. These blocks are interpreted as fragments of oceanic crust, that were mechanically separated from the slab and entrained into a channel of exhuming material, dominated by buoyant serpentinite (Shreve and Cloos, 1986; Engi et al., 2001; Gerya et al., 2002; Marschall et al., 2006b). The exhumation channel is located above the surface of the subducting slab and is, therefore, steadily fluxed and hydrated at various depths by fluids expelled from dehydrating sediments, AOC and serpentinites in the slab. Re-hydration and addition of fluid-mobile trace elements into exhuming eclogites at various pressures is, therefore, expected.

For the island of Syros, where meta-igneous blocks are enclosed in chlorite-rich schists, fluid flux and trace-element redistribution has been modelled and documented in natural samples (Bröcker and Enders, 2001; Breeding et al., 2004; Marschall et al., 2006b; Ague, 2007). The chlorite schists show a strong enrichment in Li (abundances of 30 to 80 μg/g) introduced by fluids during exhumation of the sequence (Marschall, 2005; Marschall et al., 2006a). This retrograde influx of Li-rich fluids most likely derived from the sedimentary pile of the subducting slab would explain the high Li contents in the exhumed eclogites.

However, many HPM rocks are still significantly lighter than all sediments, and cannot be explained by a simple Li transfer process. An additional fractionation process is therefore required. Kinetic fractionation of Li isotopes by diffusion has been demonstrated for natural settings on the outcrop scale (Lundstrom et al., 2005; Teng et al., 2006). For the rocks from Syros, diffusion of Li from the Li-rich fluids in the chlorite schists into the meta-igneous blocks could have generated light-Li domains in these blocks at variable Li abundances. This mechanism provides a realistic explanation for negative δ^7Li values in orogenic eclogites occurring as blocks, lenses or layers in Li-rich country rocks. A detailed discussion of the diffusion model will be presented in a future contribution.

The Trescolmen eclogite bodies, embedded in Li-rich meta-sediments (garnet-mica schists; $[\text{Li}]\leq75$ μg/g and $\delta^7\text{Li}\approx+2.7$‰ in phengite), which were investigated in the study of Zack et al. (2003) show multiple evidence for fluid flux between the metasedimentary country rock and the eclogite blocks. Formation of phengite, paragonite and amphibole together with a shift of δ^{18}O values at the margins of the blocks shows the influx of fluid from the sediments into the eclogite blocks (Wiesli et al., 2001; Zack et al., 2001, 2002, 2003; Zack and John, 2007). Cs/Rb signatures in the margin zones of the eclogite blocks can only be explained by open-system fluid exchange (Zack et al., 2001). However, Zack et al. (2003) argued that the light Li found in the eclogites could not have originated in the surrounding meta-sediments. Considering the effects of kinetic fractionation changes the discussion. Diffusive influx of Li into the eclogite blocks would indeed produce extremely light Li compositions along with elevated Li abundances.

6.4. Consequences for geochemical lithium cycling in the mantle

The results of modelling presented above show that dehydration of oceanic crust decreases the δ^7Li value by ~3‰ from the onset of metamorphism to the eclogite facies stage, along with a decrease in Li concentrations of ~40%. Average AOC will be decreased from 7.6 µg/g to 4.3 µg/g and $\delta^7\text{Li} \approx +7$‰. The global weighted mean sediment composite will decrease from 43.3 µg/g to 24.6 µg/g and $\delta^7\text{Li} \approx 0$‰. The Li budget of a subducting slab composed of these two reservoirs plus unaltered magmatic rocks ([Li] ≈ 5 µg/g; $\delta^7\text{Li} \approx +4$‰) and serpentinites ([Li] ≈ 3.5 µg/g; $\delta^7\text{Li} \approx +7.7$‰) reveals a composition very close to fresh basalts and isotopically hardly distinguishable from the mantle. A slab consisting of sediment, AOC and serpentinite (500 m each) and 5000 m of unaltered magmatic rocks would have an average Li concentration of 6.3 µg/g with $\delta^7\text{Li} = +3.1$‰. Oceanic slabs deeply subducted into the mantle may, therefore, not create Li isotopic inhomogeneities that could be detected in ocean island volcanic rocks or enriched MORB. The exact Li isotopic composition will be dependent on the relative proportions of sediments, AOC, unaltered igneous rocks and serpentinite, and the type of sediments (e.g. low-Li carbonates or high-Li clays). Clay-rich sediments, however, carry characteristic elemental (e.g. high Th/Ba) and isotopic (e.g. Pb) signatures (Plank and Langmuir, 1993; Elliott, 2003). Their contribution to the source region of mantle-derived magmas can thus be estimated using those signatures.

High Li concentrations in eclogites are most likely caused by peak-pressure or retrograde influx of Li derived from sediments with δ^7Li values between 0 and +4‰. Extremely light Li in orogenic eclogites may be explained by kinetic fractionation of Li isotopes during enrichment of eclogite blocks by diffusion from the country rocks into the eclogite blocks. This model predicts the light-Li eclogites to occur only in a restricted zone within the HPM blocks or layers. It also predicts a transient character of the light-Li zone in the blocks, as continuous diffusion will equilibrate the Li isotopic composition and erase the effects of kinetic fractionation. The spatially restricted light-Li signals will, therefore, not survive global recycling processes.

In accordance with earlier models (Zack et al., 2003; Elliott et al., 2004) our model predicts the fore-arc mantle wedge to be enriched in Li with high δ^7Li values, i.e. it will be distinctly heavier than MORB or average mantle. This enriched fore-arc material maybe mechanically coupled to the slab, dragged down into the deeper mantle and finally sampled by mantle-derived basalts, such as OIB, island arc basalts (IAB) or enriched MORB (Zack et al., 2003; Elliott et al., 2006).

The majority of OIB show MORB-like Li isotope signatures (Tomascak, 2004; Elliott et al., 2004). Interestingly, in cases where they deviate from the typical MORB range, they show δ^7Li values above +4‰. In a light-Li-slab model one would expect the formation of low-δ^7Li domains in the mantle that could be sampled by ocean island volcanoes or at MOR. In the contrasting model presented here, such low-δ^7Li domains are only produced temporarily on a very small scale and would surely not survive over the time scales of global recycling. The prediction of this model is that recycled altered oceanic crust will produce heavy-Li signatures with low concentrations, while recycled sediments will have higher Li concentrations and δ^7Li values slightly below MORB, i.e. close to average continental crust. The exact Li isotopic signature of the slab will depend on particular starting compositions of the altered crust and sediment pile (lithologies, volatile contents, Li abundances) and the *P*–*T* evolution during subduction.

7. Conclusions

Previous modelling of the Li budget of subducting oceanic crust during dehydration (Zack et al., 2003) lacked the constraints on many input parameters now available (Wunder et al., 2006, 2007; Marschall et al., 2006a; Chan et al., 2006). Using these refined inputs, we show that dehydration can account for a decrease in δ^7Li of only ≤3‰, the entire prograde metamorphic process up to anhydrous eclogite stage included. We therefore find that dehydration cannot account for light Li in HPM rocks, in contrast to previous work. Eclogites in subducting slabs are predicted to contain Li at MORB-like concentrations levels, but enriched in the heavy isotope. HPM sediments, on the other hand, are expected to be enriched in Li with δ^7Li values lower than MORB. Budgeting the composition of a subducting slab from the average values of AOC, serpentinites, sediments and unaltered magmatic rocks reveals a Li concentration (6.3 µg/g) and a δ^7Li value (+3.1‰) very close to average MORB (5 µg/g; +4‰). This demonstrates that recycled oceanic crust will generate only very minor heterogeneities in terms of Li abundance and Li isotopic composition in the mantle that could be sampled by ocean island volcanoes or at MOR. In contrast, the fore-arc mantle will be strongly enriched in Li with a heavy Li isotopic composition, and recycled mantle-wedge material would produce high-δ^7Li signals in OIB and enriched MORB.

Li abundances in excess of 20 µg/g in orogenic HPM rocks of basaltic composition (eclogites) seem most reasonably explained by addition of Li after the onset of subduction, probably during eclogitisation and/or exhumation. Light δ^7Li values are likely generated by kinetic fractionation of the Li isotopes during diffusive influx of Li from the country rocks into the eclogite bodies. A consequence of this hypothesis, which will be evaluated in more detail in a future publication, is that Li found in orogenic eclogites is not representative of rocks within subducting slabs. Other fluid-mobile elements, such as Rb, Ba, Sr, B, Cl or N could be affected in the same way by processes influencing exhuming HPM rocks, but not operating in subducting slabs. The investigation of subduction-related HPM rocks has always suffered from retrogression during exhumation. In the case of Li this problem seems to be particularly vicious, due to its high diffusivity, fluid mobility and tendency to undergo kinetic isotopic fractionation.

Acknowledgements

This paper was inspired by and benefited from discussions with Rainer Altherr, Thomas Zack, John Schumacher, Kevin Klimm, Vincent van Hinsberg, Timm John, Frank Brenker, Ralf Tappert, Andre Girnis, Alan Woodland and Gerhard Brey. For technical assistance we thank Rich Abell, Chris Coath, Carolyn Taylor, Soodabeh Durali-Müller, Anna Karina Neumann, Thomas Kautz, Franz Kneissl and Jan Heliosch. We are thankful to Tatsuki Tsujimori and an anonymous reviewer for their positive and constructive comments and to Rick Carlson for the editorial handling. H.M. appreciates the motivation drawn from the works of Andreas Frege (Düsseldorf) and Jan Vetter (Berlin). This study was financially supported by a European Union Marie-Curie Fellowship awarded to HRM (ID 025844: "Isotopes in subduction zones — the metamorphic perspective"), and by the Deutsche Forschungsgemeinschaft (grant no. BR 1012/19-1), both of which are gratefully acknowledged. PPvS and analyses at Bristol were supported by NERC grant NER/C510983/1.

Appendix A. Supplementary data

Supplementary data associated with this article can be found, in the online version, at doi:10.1016/j.epsl.2007.08.005.

References

Ague, J.J., 2003. Fluid flow in the deep crust. Treat. Geochem. 3, 195–228.

Ague, J.J., 2007. Models of permeability contrasts in subduction zone mélange: implications for gradients in fluid fluxes, Syros and Tinos islands, Greece. Chem. Geol. 239, 217–227.

Becker, H., Jochum, K.-P., Carlson, R.W., 1999. Constraints from high-pressure veins in eclogites on the composition of hydrous fluids in subduction zones. Chem. Geol. 160, 291–308.

Berger, G., Schott, J., Guy, C., 1988. Behaviour of Li, Rb and Cs during basalt glass and olivine dissolution and chlorite, smectite and zeolite precipitation from seawater: experimental investigations and modelization between 50 °C and 300 °C. Chem. Geol. 71, 297–312.

Bouman, C., Elliott, T., Vroon, P.Z., 2004. Lithium inputs to subduction zones. Chem. Geol. 212, 59–79.

Breeding, C.M., Ague, J.J., Bröcker, M., 2004. Fluid-metasedimentary rock interactions in subduction-zone mélange: implications for the chemical composition of arc magmas. Geology 32, 1041–1044.

Brenan, J.M., Ryerson, F.J., Shaw, H.F., 1998. The role of aqueous fluids in the slab-to-mantle transfer of boron, beryllium, and lithium during subduction: experiments and models. Geochim. Cosmochim. Acta 62, 3337–3347.

Bröcker, M., Enders, M., 2001. Unusual bulk-rock compositions in eclogite-facies rocks from Syros and Tinos (Cyclades, Greece): implications for U-Pb zircon geochronology. Chem. Geol. 175, 581–603.

Chan, L.H., Edmond, J.M., 1988. Variation of lithium isotope composition in the marine environment: a preliminary report. Geochim. Cosmochim. Acta 52, 1711–1717.

Chan, L.H., Edmond, J.M., Thompson, G., Gillis, K., 1992. Lithium isotopic composition of submarine basalts: implications for the lithium cycle in the ocean. Earth Planet. Sci. Lett. 108, 151–160.

Chan, L.H., Edmond, J.M., Thompson, G., 1993. A lithium isotope study of hot springs and metabasalts from mid-ocean ridge hydrothermal systems. J. Geophys. Res. 98, 9653–9659.

Chan, L.H., Gieskes, J.M., You, C.-F., Edmond, J.M., 1994. Lithium isotope geochemistry of sediments and hydrothermal fluids of the Guaymas basin. Geochim. Cosmochim. Acta 58, 4443–4454.

Chan, L.H., Leeman, W.P., You, C.-F., 1999. Lithium isotopic composition of central American volcanic arc lavas: implications for modification of subarc mantle by slab-derived fluids. Chem. Geol. 160, 255–280.

Chan, L.H., Alt, J.C., Teagle, D.A.H., 2002a. Lithium and lithium isotope profiles through the upper oceanic crust: a study of seawater–basalt exchange at ODP sites 504b and 896a. Earth Planet. Sci. Lett. 201, 187–201.

Chan, L.H., Leeman, W.P., You, C.-F., 2002b. Lithium isotopic composition of Central American volcanic arc lavas: implications for modification of subarc mantle by slab-derived fluids: correction. Chem. Geol. 182, 293–300.

Chan, L.H., Leeman, W.P., Plank, T., 2006. Lithium isotopic composition of marine sediments. Geochem. Geophys. Geosys. 7. doi:10.1029/2005GC001202.

Clift, P.D., Chan, L.H., Blusztajn, J., Layne, G.D., Kastner, M., Kelley, R.K., 2005. Pulsed subduction accretion and tectonic erosion reconstructed since 2.5 Ma from the tephra record off-shore Costa Rica. Geochem. Geophys. Geosys. 6. doi:10.1029/2005GC000963.

Coogan, L.A., Kasemann, S.A., Chakraborty, S., 2005. Rates of hydrothermal cooling of new oceanic upper crust derived from lithium-geospeedometry. Earth Planet. Sci. Lett. 240, 415–424.

Decitre, S., Deloule, E., Reisberg, L., James, R., Agrinier, P., Mével, C., 2002. Behavior of Li and its isotopes during serpentinization of oceanic peridotites. Geochem. Geophys. Geosys. 3. doi:10.1029/2001GC000178.

Decitre, S., Buatier, M., James, R., 2004. Li and Li isotopic composition of hydrothermally altered sediments at Middle Valley, Juan de Fuca. Chem. Geol. 211, 363–373.

Donnelly, T.W., Thompson, G., Salisbury, M.H., 1980. The chemistry of altered basalts at site 417, Deep Sea Drilling Project leg 51. Init. Rep. DSDP 51–53, 1319–1330.

Elliott, T., 2003. Tracers of the slab, In: Eiler, J. (Ed.), Inside the Subduction Factory, 1st Edition. Geophys. Monogr. Ser. Am. Geophys, vol. 138. Union, Washington, DC, pp. 23–45.

Elliott, T., Jeffcoate, A., Bouman, C., 2004. The terrestrial Li isotope cycle: light-weight constraints on mantle convection. Earth Planet. Sci. Lett. 220, 231–245.

Elliott, T., Thomas, A., Jeffcoate, A., Niu, Y., 2006. Lithium isotope evidence for subduction-enriched mantle in the source of mid-ocean-ridge basalts. Nature 443, 565–568.

Engi, M., Berger, A., Roselle, G.T., 2001. Role of the tectonic accretion channel in collisional orogeny. Geology 29, 1143–1146.

Flesch, G.D., Anderson, A.R., Svec, H.J., 1973. A secondary isotopic standard for 6 Li/7 Li determinations. Int. J. Mass Spectrom. Ion Process. 12, 265–272.

Gerya, T.V., Stoeckhert, B., Perchuk, A.L., 2002. Exhumation of high-pressure metamorphic rocks in a subduction channel; a numerical simulation. Tectonics 21, 6–19.

James, R.H., Palmer, M.R., 2000. The lithium isotope composition of international rock standards. Chem. Geol. 166, 319–326.

James, R.H., Rudnicki, M.D., Palmer, M.R., 1999. The alkali element and boron geochemistry of the Escanaba trough sediment-hosted hydrothermal system. Earth Planet. Sci. Lett. 171, 157–169.

Jeffcoate, A.B., Elliott, T., Thomas, A., Bouman, C., 2004. Precise, small sample size determinations of lithium isotopic compositions of geological reference materials and modern seawater by MC-ICP-MS. Geostand. Geoanal. Res. 28, 161–172.

Jeffcoate, A.B., Elliott, T., Kasemann, S.A., Ionov, D., Cooper, K., Brooker, R., 2007. Li isotope fractionation in peridotites and mafic melts. Geochim. Cosmochim. Acta 71, 202–218.

John, T., Schenk, V., 2003. Partial eclogitisation of gabbroic rocks in a late Precambrian subduction zone (Zambia): prograde metamorphism triggered by fluid infiltration. Contrib. Mineral. Petrol. 146, 174–191.

John, T., Scherer, E.E., Haase, K., Schenk, V., 2004. Trace element fractionation during fluid-induced eclogitisation in a subducting slab: trace element and Lu–Hf–Sm–Nd isotope systematics. Earth Planet. Sci. Lett. 227, 441–456.

Kretz, R., 1983. Symbols for rock-forming minerals. Am. Mineral. 68, 277–279.

Li, Y.-H., Gregory, S., 1974. Diffusion of ions in sea-water and in deep-sea sediments. Geochim. Cosmochim. Acta 38, 703–714.

Lundstrom, C.C., Chaussidon, M., Hsui, A.T., Keleman, P., Zimmerman, M., 2005. Observations of Li variations in the trinity ophiolite: evidence for isotopic fractionation by diffusion during mantle melting. Geochim. Cosmochim. Acta 69, 735–751.

Marschall, H.R., 2005. Lithium, beryllium, and boron in high-pressure metamorphic rocks from Syros (Greece). Dr. rer. nat. thesis, Univ. Heidelberg, Germany. URL http://www.ub.uni-heidelberg.de/archiv/5634.

Marschall, H.R., Altherr, R., Ludwig, T., Kalt, A., Gméling, K., Kasztovszky, Zs., 2006a. Partitioning and budget of Li, Be and B in high-pressure metamorphic rocks. Geochim. Cosmochim. Acta 70, 4750–4769.

Marschall, H.R., Ludwig, T., Altherr, R., Kalt, A., Tonarini, S., 2006b. Syros metasomatic tourmaline: evidence for very high-δ^{11}B fluids in subduction zones. J. Petrol. 47, 1915–1942.

Marschall, H.R., Altherr, R., Rüpke, L., 2007. Squeezing out the slab — modelling the release of Li, Be and B during progressive high-pressure metamorphism. Chem. Geol. 239, 323–335.

Moriguti, T., Nakamura, E., 1998. Across-arc variation of Li-isotopes in lavas and implications for crust/mantle recycling at subduction zones. Earth Planet. Sci. Lett. 163, 167–174.

Niu, Y., 2004. Bulk-rock major and trace element compositions of abyssal peridotites: implications for mantle melting, melt extraction and post-melting processes beneath ocean ridges. J. Petrol. 45, 2423–2458.

Parkinson, I.J., Hammond, S.J., James, R.H., Rogers, N.W., 2007. High-temperature lithium isotope fractionation: insights from lithium isotope diffusion in magmatic systems. Earth Planet. Sci. Lett. 257, 609–621.

Plank, T., Langmuir, C.H., 1993. Tracing trace elements from sediment input to volcanic output at subduction zones. Nature 362, 739–742.

Pogge von Strandmann, P.A.E., Burton, K.W., James, R.H., van Calsteren, P., Gíslason, S.R., Mokadem, F., 2006. Riverine behaviour of uranium and lithium isotopes in an actively glaciated basaltic terrain. Earth Planet. Sci. Lett. 251, 134–147.

Richter, F.M., Davis, A.M., DePaolo, D.J., Watson, E.B., 2003. Isotope fractionation by chemical diffusion between molten basalt and rhyolite. Geochim. Cosmochim. Acta 67, 3905–3923.

Richter, F.M., Mendybaev, R.A., Christensen, J.N., Hutcheon, I.D., Williams, R.W., Sturchio, N.C., Beloso Jr., A.D., 2006. Kinetic isotopic fractionation during diffusion of ionic species in water. Geochim. Cosmochim. Acta 70, 277–289.

Ryan, J.G., Langmuir, C.H., 1987. The systematics of lithium abundances in young volcanic rocks. Geochim. Cosmochim. Acta 51, 1727–1741.

Scambelluri, M., Müntener, O., Ottolini, L., Pettke, T.T., Vanucci, R., 2004. The fate of B, Cl and Li in subducted oceanic mantle and in the antigorite breakdown fluids. Earth Planet. Sci. Lett. 222, 217–234.

Schmidt, M.W., Vielzeuf, D., Auzanneau, E., 2004. Melting and dissolution of subducting crust at high pressures: the key role of white mica. Earth Planet. Sci. Lett. 228, 65–84.

Seitz, H.-M., Brey, G.P., Lahaye, Y., Durali, S., Weyer, S., 2004. Lithium isotopic signatures of peridotite xenoliths and isotopic fractionation at high temperature between olivine and pyroxenes. Chem. Geol. 212, 163–177.

Shreve, R.L., Cloos, M., 1986. Dynamics of sediment subduction, melange formation, and prism accretion. J. Geophys. Res. 91, 10229–10245.

Spandler, C., Hermann, J., 2006. High-pressure veins in eclogite from New Caledonia and their significance for fluid migration in subduction zones. Lithos 89, 135–153.

Teng, F.-Z., McDonough, W.F., Rudnick, R.L., Dalpé, C., Tomascak, P.B., Chappell, B.W., Gao, S., 2004. Lithium isotopic composition and concentration of the upper continental crust. Geochim. Cosmochim. Acta 68, 4167–4178.

Teng, F.-Z., McDonough, W.F., Rudnick, R.L., 2006. Diffusion-driven extreme lithium isotopic fractionation in country rocks of the Tin Mountain pegmatite. Earth Planet. Sci. Lett. 243, 701–710.

Teng, F.-Z., McDonough, W.F., Rudnick, R.L., Wing, B.A., 2007. Limited lithium isotopic fractionation during progressive metamorphic dehydration in metapelites: a case study from the Onawa contact aureole, Maine. Chem. Geol. 239, 1–12.

Tomascak, P.B., 2004. Developments in the understanding and application of lithium isotopes in the earth and planetary sciences. In: Johnson, C.M., Beard, B.L., Albarède, F. (Eds.), Geochemistry of Non-Traditional Stable Isotopes. . Rev. Mineral. Mineral. Soc. Am., vol. 55. Mineralogical Society of America, Washington, DC, pp. 153–195. Ch. 5.

Tomascak, P.B., Ryan, J.G., Defant, M.J., 2000. Lithium isotope evidence for light element decoupling in the Panama subarc mantle. Geology 28, 507–510.

Vils, F., Pelletier, L., Kalt, A., Ludwig, T., 2007. Light element input to subduction zones; results from ODP leg 209 peridotites. Geophys. Res. Abstr. 9, 09498.

Widmer, T., Thompson, A.B., 2001. Local origin of high-pressure vein material in eclogite facies rocks of the Zermatt-Saas zone, Switzerland. Am. J. Sci. 301, 627–656.

Wiesli, R.A., Taylor, L.A., Valley, J.W., Trommsdorff, V., Kurosawa, M., 2001. Geochemistry of eclogites and metapelites from Trescolmen, Central Alps, as observed from major and trace elements and oxygen isotopes. Int. Geol. Rev. 43, 95–119.

Williams, L.B., Hervig, R.L., 2005. Lithium and boron isotopes in illite–smectite: the importance of crystal size. Geochim. Cosmochim. Acta 69, 5705–5716.

Woodland, A.B., Seitz, H.-M., Altherr, R., Olker, B., Marschall, H., Ludwig, T., 2002. Li abundances in eclogite minerals: a clue to a crustal or mantle origin? Contrib. Mineral. Petrol. 143, 587–601 Erratum: Contrib. Mineral. Petrol. 144, 128–129.

Wunder, B., Meixner, A., Romer, R.L., Heinrich, W., 2006. Temperature-dependent isotopic fractionation of lithium between clinopyroxene and high-pressure fluids. Contrib. Mineral. Petrol. 151, 112–120.

Wunder, B., Meixner, A., Romer, R.L., Feenstra, A., Schettler, G., Heinrich, W., 2007. Lithium isotope fractionation between Li-bearing staurolite, Li-mica and aqueous fluids: an experimental study. Chem. Geol. 238, 277–290.

Zack, T., John, T., 2007. An evaluation of reactive fluid flow and trace element mobility in subducting slabs. Chem. Geol. 239, 199–216.

Zack, T., Rivers, T., Foley, S.F., 2001. Fluid infiltration at 2.0 GPa in eclogites from Trescolmen, Central Alps: constraints from Cs–Rb–Ba systematics in phengites and amphiboles. Contrib. Mineral. Petrol. 140, 651–669.

Zack, T., Foley, S.F., Rivers, T., 2002. Equilibrium and disequilibrium trace element partitioning in hydrous eclogites (Trescolmen, Central Alps). J. Petrol. 43, 1947–1974.

Zack, T., Tomascak, P.B., Rudnick, R.L., Dalpe, C., McDonough, W.F., 2003. Extremely light Li in orogenic eclogites: the role of isotope fractionation during dehydration in subducted oceanic crust. Earth Planet. Sci. Lett. 208, 279–290.